



## Brief Communication

# Analytical solutions for the axisymmetric flow inside a cylindrical container with a rod along the axis at low Reynolds numbers

Juan Carlos Sturzenegger, Luis G. Sarasúa, Arturo C. Martí\*

Instituto de Física, Iguá 4225, Universidad de la República, 11400 Montevideo, Uruguay

## ARTICLE INFO

## Article history:

Received 1 June 2010

Accepted 2 November 2011

Available online 26 November 2011

## Keywords:

Vortex breakdown

Recirculation flow

Control

## ABSTRACT

The axisymmetric flow inside a cylindrical container with a rod along its symmetry axis is studied. The flow is produced by the rotation of one of the cylinder end walls, of both end walls, or of the sidewall. Analytical expressions (for low Reynolds numbers) of the azimuthal velocity field are presented, thus extending the solutions of the case without rod. Graphics of constant azimuthal velocity lines are obtained for two configurations (both end walls in rotation, one end wall in rotation). The calculations are based on summations with different number of terms. The introduction of Lanczos factors in the summations is shown to play an important role improving their convergence.

© 2011 Elsevier Ltd. All rights reserved.

## 1. Introduction

The dynamics of viscous and incompressible flows inside cylindrical containers with rotating end or lateral walls has received considerable attention (Brown and López, 1990; Khalili and Rath, 1994; López, 1990, 1995, 1996). Analytical solutions of the flow inside the container are not possible in general but only in some special cases (Khalili and Rath, 1994; Pao, 1972; Schmeiden, 1928; Schultz-Grunow, 1935). In this contribution we present an example in which an analytical solution can be calculated.

One of the first studies of the flow produced by a rotating disk inside a cylindrical container was made by Schultz-Grunow (1935). That work includes an analytical solution of the flow without satisfying the non-slip boundary conditions on the container sidewall. The obtained solution is rather close to the experimental results when the aspect ratio  $\delta = H/R$  (where  $H$  and  $R$  are respectively the container height and radius) is very small. It is also worth mentioning that analytical solutions of the flow in a cylindrical container which verify all the boundary conditions but with the restriction that the Reynolds number is small have been obtained in previous works by Schmeiden (1928), Pao (1972), Khalili and Rath (1994), Muite (2004) and Cao et al. (2010).

The dynamics of closed flows inside cylindrical containers is relevant not only from an academic point of view. Indeed, for certain values of the characteristic parameters, when the swirl is sufficiently large, vortex breakdown (VB) occurs. This phenomenon is characterized by the appearance of a stagnation point near the axis, followed by regions of reversed axial flow with a bubble structure. This structural transformation is also accompanied by a sudden change of the core size and the appearance of disturbances located downstream of the core enlargement. Several experimental studies on this phenomenon have been performed, one of the most outstanding is that of Escudier (1984). As it can be seen in that article, depending on the parameters VB produces one, two, or three recirculating bubbles at the symmetry axis.

\* Corresponding author. Tel.: +598 25258624; fax: +598 25250580.

E-mail address: [marti@fisica.edu.uy](mailto:marti@fisica.edu.uy) (A.C. Martí).

Due to the great number of practical implications of VB, the development of mechanisms for controlling its emergence is of considerable interest. The introduction of a cylindrical rod along the symmetry axis is one of the methods used to control the flow and the appearance of VB.

There are several experimental articles in which the behavior of VB is studied when adding a cylindrical rod (which can be straight or slightly conical), see, for instance, Mullin et al. (2000), Husain et al. (2003), and Cabeza et al. (2010). In the work by Mullin et al. (2000), the effect of adding a small rod along the axis of the cylinder is shown to be robust despite the qualitative change in the boundary conditions. It is also reported that sloping the inner cylinder has a dramatic effect enhancing or suppressing the recirculation. The approach to control VB presented by Husain et al. (2003) is based on the addition of co- or counter-rotation near the axis using a small central rod rotating independently of the bottom or rotating end wall. It is concluded that such a method may be an effective way to either enhance or suppress VB. More recently, using a device which does not require the addition of swirl near the axis (and therefore is more feasible in engineering devices), Cabeza et al. (2010) have shown that the rod may increase or decrease the critical Reynolds number for the emergence of VB depending on the aspect ratio and the radius of the rod.

Other approaches to the control of VB are based on the introduction of a small rotating disk in the end wall opposite to the rotating wall (Mununga et al., 2004; Yu et al., 2006, 2007), or the use of axial temperature gradients (Herrada and Shtern, 2003). More recently, Lo Jacono et al. (2008) studied the effect of the length of the rod. In coincidence with other previous results, they found that for large rods the co-rotation suppresses VB, unlike counter-rotation which enhances VB region. On the other hand, for short rod lengths, the behavior of the recirculation zone is more complex and as the rod shortens, the behavior approaches the limit of a flat disk and the recirculation zone bubble vanishes for sufficient counter-rotation speed.

In this paper we extend previous analytical solutions of the flow inside a cylindrical container to the case in which a small stationary rod is placed along the axis. Moreover, we study the convergence of the series and the influence of the so-called Lanczos factors. Firstly, in Section 2 we formulate the problem and present its solution in the classical configuration without rod. Next, in Section 3 we obtain the analytical solution to the problem with rod. The velocity fields are presented in Section 4 for some particular cases. Finally, in Section 5, we present a summary and the conclusion.

## 2. Problem formulation without rod

We consider the flow in a cylinder of radius  $R$  and height  $H$  with top, bottom and lateral walls either at rest or rotating with arbitrary angular velocities. The cylinder is filled with fluid of constant kinematic viscosity  $\nu$ . In the case of one single angular velocity  $\Omega$ , the two dimensionless numbers that characterize this problem are the Reynolds number  $Re = \Omega R^2 / \nu$  and the aspect ratio  $\delta = H/R$ .

In this study, as it is restricted to low Reynolds numbers, we assume that the flow is axisymmetric (Brown and López, 1990; López, 1990). Then, the flow is governed by the axisymmetric Navier–Stokes equations which can be written using a cylindrical polar coordinate system  $(r, \theta, z)$  whose symmetry axis coincides with the axis of the cylinder. The corresponding velocity field is denoted as  $v_r, v_\theta, v_z$ , and the pressure as  $p$ . We make the governing equations non-dimensional by scaling the radius of the cylinder and one characteristic angular velocity. Then the top and bottom wall are located at  $z=0$  and  $z=\delta$  while the sidewall is located at  $r=1$ . Through all this work we consider non-slip boundary conditions. Moreover, the introduction of the stream function  $\psi$  where  $v_r = -(1/r)\partial\psi/\partial z$ , and  $v_z = (1/r)\partial\psi/\partial r$  will prove to be useful.

Broadly speaking, the rotation of the cylinder lid has the following effects. The fluid inside the cylinder in the vicinity of the moving disk is driven by it towards the periphery, in a spiral movement (with azimuthal and radial components). On the other hand, there is also an axial and radial recirculation: the fluid moves axially inside the cylinder along the periphery from the region near the rotating disk into the region near the opposite disk. In this latter region, it moves radially from the periphery towards the center. It then continues moving along the symmetry axis towards the region near the rotating disk, completing the cycle. The conservation of angular momentum causes the fluid driven towards the symmetry axis to increase its angular velocity, creating a vortex along the axis.

An analytical solution for the flow inside the cylindrical container – when VB has not yet taken place – is given by Muite (2004). Using asymptotic expansions in  $Re$ , it can be obtained (Hills, 2001)

$$v_\theta = v_{\theta,0} + (Re)v_{\theta,1} + (Re)^2 v_{\theta,2} + \dots, \quad (1)$$

and similar expansions for the stream function. These expressions are replaced in the Navier–Stokes equations and discriminated for different orders of  $Re$ . The zero-order flow equations, which have only azimuthal component, are obtained. Thus,  $\psi_0 = 0$  and

$$\frac{1}{\delta^2} \frac{\partial^2 v_{\theta,0}}{\partial z^2} + \frac{\partial^2 v_{\theta,0}}{\partial r^2} + \frac{1}{r} \frac{\partial v_{\theta,0}}{\partial r} - \frac{v_{\theta,0}}{r^2} = 0. \quad (2)$$

We write hereafter  $z$  instead of  $z/\delta$ . The zero-order analytical solution is obtained

$$v_{\theta,0} = zr + 2 \sum_{n=1}^{\infty} \frac{\sin[n\pi(z-1)] I_1[\lambda_n r]}{n\pi I_1[\lambda_n]}, \quad (3)$$

where  $I_1$  is the first-order modified Bessel function of the first kind and  $\lambda_n = n\pi/\delta$ . The flow first-order analytical solution can be similarly obtained (Muite, 2004).

In those systems with sliding walls, there is a discontinuity in the flow in the periphery of the rotating lid as the sidewall is at rest. The lid drags the fluid next to it and the sidewall, on the other hand, imposes low velocities in the fluid nearby. Muite (2004) has also considered how this affects discontinuity in the analytical solutions found. The discontinuous boundary conditions reduce the convergence rate of series solutions, and to get a physically reasonable solution of the velocity field, the conditions along the discontinuous edge cannot be modeled as a discontinuous jump.

One solution is to truncate the series representation. But simple truncation does not assure that the result is an accurate representation of the velocity field. In a trigonometric expansion, a procedure that results in a truncated series expansion that approximates the required function is the implementation of the so-called Lanczos correction factors (Lanczos, 1956; Muite, 2004). These factors replace the discontinuous velocity jump by a region of rapid transition that preserves the properties of the solution away from the discontinuity. The resulting zero-order solutions are

$$v_{\theta,0} = zr + 2 \sum_{n=1}^k \frac{\sin[n\pi(z-1)] I_1[\lambda_n r] \sin\left[\frac{n\pi}{k}\right]}{n\pi I_1[\lambda_n] \frac{n\pi}{k}} \tag{4}$$

In a somewhat similar approach Khalili and Rath (1994) have also considered this problem. Under the assumptions of axisymmetry and that the radial and axial components of flow velocities are small compared to the azimuthal component  $v_r \ll v_\theta$ ,  $v_z \ll v_\theta$ , which meets approximately reality when  $Re \leq 10$ , using the Navier–Stokes equations, the azimuthal equation takes the form

$$\delta^2 \left( \frac{\partial^2 v}{\partial r^2} + \frac{1}{r} \frac{\partial v}{\partial r} - \frac{v}{r^2} \right) + \frac{\partial^2 v}{\partial z^2} = 0, \tag{5}$$

where  $v = v_\theta/R\omega$  is the azimuthal dimensionless velocity. This equation is solved by substituting the following kind of solution

$$v(r,z) = [(s-1)z+1]r + f_1(z)f_2(r), \tag{6}$$

and separating variables. The lower lid and the upper lid rotate respectively with angular velocities  $\omega_1$  and  $\omega_2$ , and the parameter  $s = \omega_2/\omega_1$  is introduced. Solving the two ordinary differential equations obtained for  $f_1(z)$  and  $f_2(r)$  the analytical solution is obtained

$$v(r,z) = [(s-1)z+1]r + \sum_{n=1}^{\infty} A_n I_1(\lambda_n r) \sin(n\pi z), \tag{7}$$

where the coefficients  $A_n$  take the following form

$$A_n = \frac{2}{n\pi I_1(\lambda_n)} [s(-1)^n - 1]. \tag{8}$$

This problem can be generalized to the case in which the lower lid, the upper lid, and the sidewall rotate respectively with angular velocities  $\omega_1$ ,  $\omega_2$  and  $\omega_3$ . The parameters  $s_1 = \omega_1/\omega$ ,  $s_2 = \omega_2/\omega$  and  $s_3 = \omega_3/\omega$  are defined, where  $\omega$  is some characteristic angular velocity. In that case, Eqs. (7) and (8) take the following forms

$$v(r,z) = [(s_2-s_1)z+s_1]r + \sum_{n=1}^{\infty} A_n I_1(\lambda_n r) \sin(n\pi z), \tag{9}$$

$$A_n = \frac{2}{n\pi I_1(\lambda_n)} [(s_2-s_3)(-1)^n + (s_3-s_1)]. \tag{10}$$

### 3. Solution with rod along the axis

The objective of our work is to obtain analytical solutions of the Stokes flow inside the cylindrical container, but with the addition of a cylindrical rod which coincides with the cylinder symmetry axis. The rod extends from  $z=0$  to  $z=1$ , and its radius is  $r=d < 1$ . Under the assumptions of axisymmetry and of radial and axial flow components being small compared to the azimuthal component, Eq. (5) is still valid but the boundary conditions are different. In this case, the analytical solution can be written as

$$v(r,z) = [(s-1)z+1]r + \sum_{n=1}^{\infty} [A_n I_1(\lambda_n r) + B_n K_1(\lambda_n r)] \sin(n\pi z), \tag{11}$$

where also appears  $K_1$ , the first-order modified Bessel function of the second kind. The parameter  $s$  is the same one as in Eq. (7).

So as to complete the search of the velocity field solutions, it is necessary to calculate the coefficients  $A_n$  and  $B_n$  using the boundary conditions. Taking the last equation into account, at the top ( $z=1$ ) and bottom ( $z=0$ ) walls the boundary conditions are always satisfied. From the boundary conditions at the rod,  $r=d$ , and the sidewall  $r=1$  ( $0 < z < 1$ ) and projecting these two equations on the function family  $\sin(n\pi z)$  the coefficients  $A_n$  and  $B_n$  can be easily derived

$$A_n = \frac{2}{n\pi} [s(-1)^n - 1] \frac{K_1(\lambda_n d) - K_1(\lambda_n) d}{I_1(\lambda_n) K_1(\lambda_n d) - I_1(\lambda_n d) K_1(\lambda_n)}, \tag{12}$$

$$B_n = \frac{2}{n\pi} [s(-1)^n - 1] \frac{I_1(\lambda_n d) - I_1(\lambda_n) d}{K_1(\lambda_n) I_1(\lambda_n d) - K_1(\lambda_n d) I_1(\lambda_n)}. \tag{13}$$

This problem can be also generalized to the case where the lower lid, the upper lid and the lateral wall are rotating with different angular velocities. Using the same notation of the previous section, in this case, Eq. (11) takes the following form

$$v(r, z) = [(s_2 - s_1)z + s_1]r + \sum_{n=1}^{\infty} [A_n I_1(\lambda_n r) + B_n K_1(\lambda_n r)] \sin(n\pi z). \tag{14}$$

The coefficients  $A_n$  and  $B_n$  can be analogously found

$$A_n = \frac{2}{n\pi} [(s_2 - s_3)(-1)^n + s_3 - s_1] \frac{K_1(\lambda_n d) - K_1(\lambda_n) d}{I_1(\lambda_n) K_1(\lambda_n d) - I_1(\lambda_n d) K_1(\lambda_n)}, \tag{15}$$

$$B_n = \frac{2}{n\pi} [(s_2 - s_3)(-1)^n + s_3 - s_1] \frac{I_1(\lambda_n d) - I_1(\lambda_n) d}{K_1(\lambda_n) I_1(\lambda_n d) - K_1(\lambda_n d) I_1(\lambda_n)}. \tag{16}$$

### 4. Velocity fields

In this section we use Eq. (14) to calculate the azimuthal velocity field inside the cylindrical cavity with two lids and a rod along its axis corresponding to two configurations. The calculated velocity fields are compared with those of the case where there is no rod along the axis studied by Khalili and Rath (1994).

The first configuration, shown in Figs. 1 and 2, corresponds to both lids in rotation with the same angular velocity ( $s_1 = s_2 = 1$ ), and still sidewall ( $s_3 = 0$ ). These conditions are imposed on Eqs. (9) and (14) respectively in both cases (with and without rod along the axis). As the calculations cannot be performed with infinite terms, the summations must be truncated at a certain  $k$ . It is expected that for some  $k$ , the truncated summation will be fairly close to the infinite summation. After several tests, it was found that when taking 50 terms, smooth lines of azimuthal velocity field are

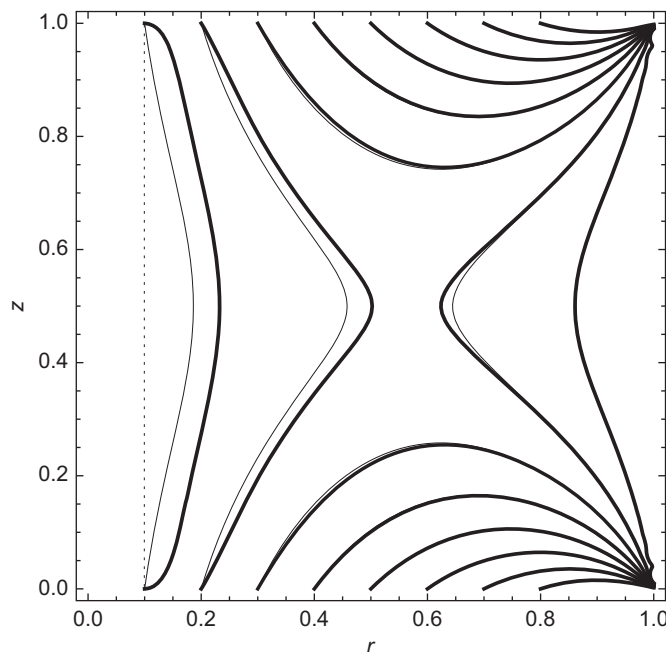


**Fig. 1.** Constant azimuthal velocity lines, for  $s_1 = 1$ ,  $s_2 = 1$ ,  $s_3 = 0$ , and  $\delta = 1$ ; calculated as a summation of 50 terms, for the cases with rod (thick lines) and without rod (thin lines). The values of azimuthal velocity on the lines are equally spaced, ranging from 0.1 to 0.8, and  $d = 0.1$ .

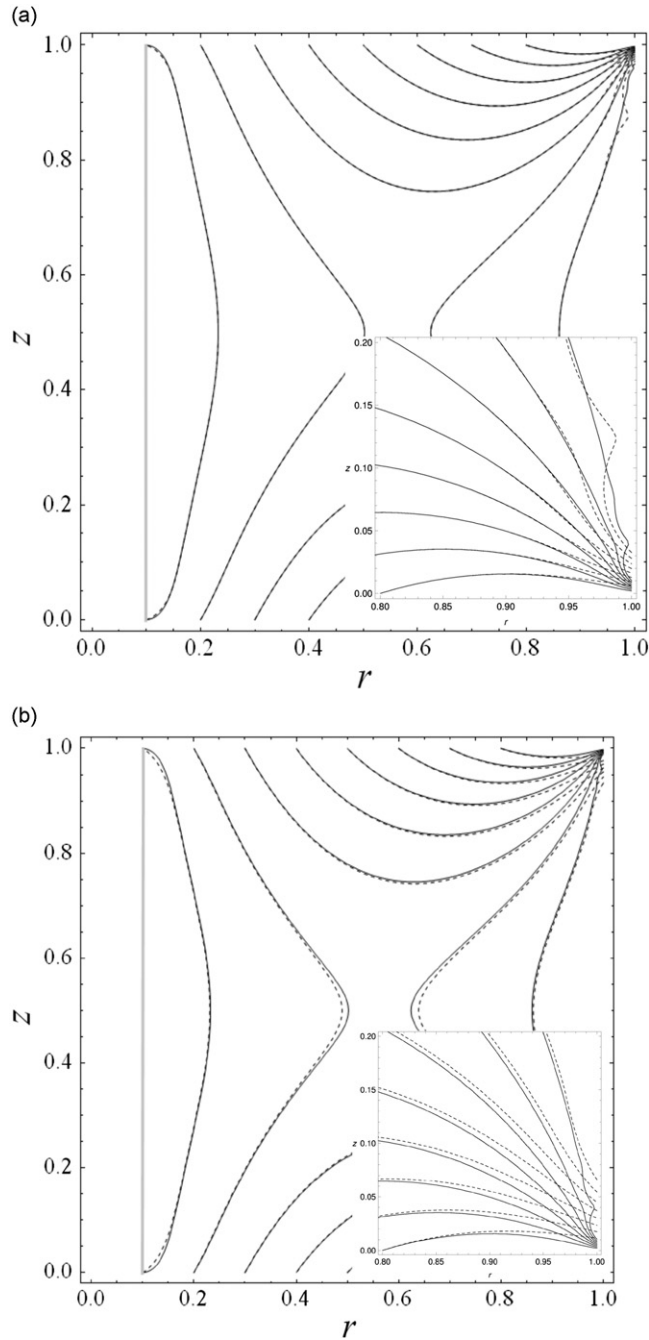


**Fig. 2.** Case with rod at the axis. Constant azimuthal velocity lines for  $s_1 = 1$ ,  $s_2 = 1$ ,  $s_3 = 0$ , and  $\delta = 1$ ; calculated without Lanczos factors for 15 (dashed lines) and 50 (solid lines) terms of the series expansion (a) and calculated as a summation of 50 terms without Lanczos factors and 15 terms with Lanczos factors (b). The insets show details in the region around the corner.

obtained, as expected. These are similar to those presented in the paper by Khalili and Rath (1994). The graphics obtained can be seen in Fig. 1 in which both cases (with and without rods) are superimposed. In this figure we can observe that most of the lines match, except for the lines with small  $v$  near the symmetry axis, which, in the case with rod, move away from that axis.

In Fig. 2(a) we can see the velocity fields corresponding to the case with rod, with  $k=15$  and  $k=50$  superimposed. The irregularities in the lines of constant azimuthal velocity near  $(r; z) = (1; 0)$  and  $(r; z) = (1; 1)$  clearly increase when  $k=15$ .

The next step is to introduce the so-called Lanczos factors which replace the discontinuous velocity jumps by a region of rapid transition that preserves the properties of the solution away from the discontinuity (Muite, 2004). In the case

without rod along the axis the expression reads as

$$v(r,z) = r + \sum_{n=1}^k A_n I_1(\lambda_n r) \sin(n\pi z) \frac{\sin(\frac{n\pi}{k})}{\frac{n\pi}{k}}, \quad (17)$$

while in the case with rod along the axis as

$$v(r,z) = r + \sum_{n=1}^k [A_n I_1(\lambda_n r) + B_n K_1(\lambda_n r)] \sin(n\pi z) \frac{\sin(\frac{n\pi}{k})}{\frac{n\pi}{k}}. \quad (18)$$

As expected, the introduction of Lanczos factors reduces the irregularities in the lines of constant azimuthal velocity near  $(r; z) = (1; 0)$  and  $(r; z) = (1; 1)$ , which is noticed specially when graphics with  $k=15$  with Lanczos factors and  $k=50$  without Lanczos factors (the latter considered close to the real field) are superimposed (Fig. 2(b)). Thus, it can be seen that Lanczos factors smooth velocity lines, but these are a little separated from real values in the regions near  $(r; z) = (1; 0)$  and  $(r; z) = (1; 1)$ . It should be noted that there is also a small discrepancy in the middle region ( $r \sim 0.5$ ,  $z \sim 0.5$  for  $k=15$ ), therefore the effect of the Lanczos factors can be favorable or not, depending on the region of the flow.

For the second configuration, with the lower lid in rotation and the top lid fixed, the conditions  $s_1 = 1$ ,  $s_2 = s_3 = 0$  and  $\delta = 1$  are imposed on Eqs. (9) and (14). Similarly to the previous case the infinite summations must be truncated at a certain  $k$  obtaining in the case without rod

$$v(r,z) = [-z+1]r + \sum_{n=1}^k A_n I_1(\lambda_n r) \sin(n\pi z), \quad (19)$$

and in the case with rod along the axis

$$v(r,z) = [-z+1]r + \sum_{n=1}^k [A_n I_1(\lambda_n r) + B_n K_1(\lambda_n r)] \sin(n\pi z). \quad (20)$$

Following the previous procedure, it was found that when taking 50 terms, smooth lines for the azimuthal velocity field were obtained. In Fig. 3 the results corresponding to both cases (with and without rods) are superimposed, this shows that most of the lines match, except for the lines with small  $v$  near the symmetry axis, which in the case with rod move away from that axis.

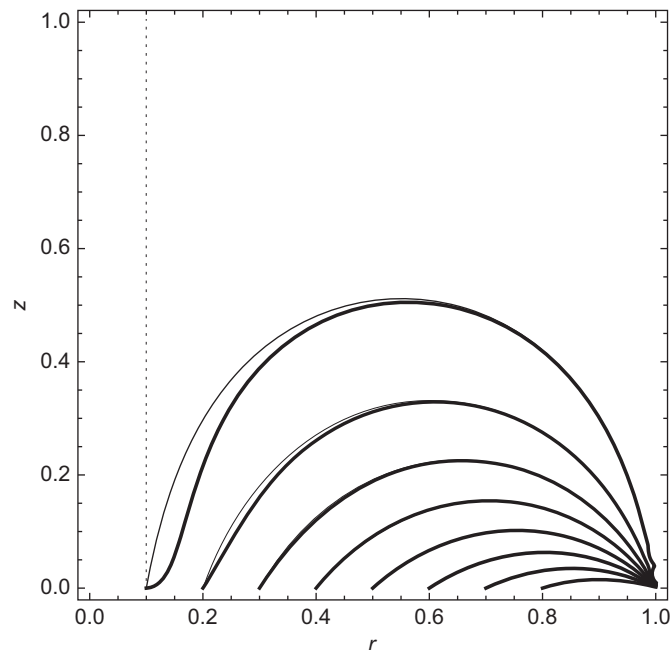


**Fig. 3.** Constant azimuthal velocity lines, for  $s_1 = 1$ ,  $s_2 = 0$ ,  $s_3 = 0$ , and  $\delta = 1$ ; calculated as a summation of 50 terms. Thin lines: configuration without rod; thick lines: configuration with rod ( $d = 0.1$ ). The values of azimuthal velocity on the lines are equally spaced, ranging from 0.1 to 0.8.

## 5. Conclusion

In this paper we have obtained analytical expressions for the Stokes flow of the azimuthal velocity field inside a cylindrical container with lids, with a cylindrical rod along its axis. We have thus extended the analytical solutions obtained by Khalili and Rath (1994) and Muite (2004) including the addition of a rod along the cylinder axis.

We have obtained graphics of constant azimuthal velocity lines for two configurations (both lids in rotation, one of the lids in rotation) based on summations with different number of terms. We found that 50 terms are enough to obtain good accuracy. When the number of terms is reduced, there appear defects in the lines.

We have also found that the use of Lanczos factors smoothes constant velocity lines reducing defects. Thus lines of good accuracy throughout the domain of  $(r; z)$  values can be obtained, except in the vicinity of singular points  $(1; 0)$  and  $(1; 1)$ . With 15 terms and the use of Lanczos factors, we obtained similar results (except near singular points) to those we obtained with 50 terms without Lanczos factors.

Moreover, when inspecting the graphics where constant velocity lines corresponding to configurations with and without rods are superimposed, it can be seen that they match in almost all the domain of  $(r; z)$  values, except in the region near the cylinder symmetry axis ( $r = 0$ ). Thus we see that the effect of the modification in the boundary conditions is quite large near the rod. This result, in the limit of low Reynolds numbers, could be related to the experimental observation that for intermediate  $Re$ , the boundary layer generation near the rod can significantly influence the local flow, and particularly, VB and the necessary  $Re$  to obtain it, in spite of the fact that the overall flow is not drastically modified (Cabeza et al., 2010).

Finally, it is worth emphasizing the present approach could be extended to different setups, for example, a rod rotating (Husain et al., 2003), instead of being at rest, or a small disk rotating near the end wall opposite to the rotating wall (Mununga et al., 2004). We hope that obtaining analytical expressions for the solutions in those cases will contribute to a better understanding and control of VB phenomena.

## Acknowledgments

We thank the anonymous reviewers for their careful and thoughtful reading. We acknowledge financial support from PEDECIBA and CSIC (Uruguay).

## References

- Brown, G.L., López, J.M., 1990. Axisymmetric vortex breakdown. Part 2. Physical mechanisms. *Journal of Fluid Mechanics* 221, 553–576.
- Cabeza, C., Sarasúa, L.G., Martí, A.C., Bove, I., Varela, S., Usera, G., Vernet, A., 2010. Influence of coaxial cylinders on vortex breakdown in a closed flow. *European Journal of Mechanics B/Fluids* 29, 201–207.
- Cao, S., Ozono, S., Tamura, Y., Ge, Y., Kikugawa, H., 2010. Numerical simulation of Reynolds number effects on velocity shear flow around a circular cylinder. *Journal of Fluids and Structures* 26, 685–702.
- Escudier, M.P., 1984. Observations of the flow produced in a cylindrical container by a rotating endwall. *Experiments in Fluids* 2, 189–196.
- Herrada, M.A., Shtern, V., 2003. Vortex breakdown control by adding near-axis swirl and temperature gradients. *Physical Review E* 68, 041202.
- Hills, C.P., 2001. Eddies induced in cylindrical containers by a rotating endwall. *Physics of Fluids* 13, 2279–2286.
- Husain, H.S., Shtern, V., Hussain, F., 2003. Control of vortex breakdown by addition of near-axis swirl. *Physics of Fluids* 15, 271–279.
- Khalili, A., Rath, H.J., 1994. Analytical solution for a steady flow of enclosed rotating disks. *Zeitschrift für Angewandte Mathematik und Physik* 45, 670–680.
- Lanczos, A., 1956. *Applied Analysis*. Prentice Hall, Englewood Cliffs.
- Lo Jacono, D., Sørensen, J.N., Thompson, M.C., Hourigan, K., 2008. Control of vortex breakdown in a closed cylinder with a small rotating rod. *Journal of Fluids Structures* 24, 1278–1283.
- López, J.M., 1990. Axisymmetric vortex breakdown. Part 1. Confined swirling flow. *Journal of Fluid Mechanics* 221, 533–552.
- López, J.M., 1995. Unsteady swirling flow in an enclosed cylinder with reflectional symmetry. *Physics of Fluids* 7, 2700–2714.
- López, J.M., 1996. Flow between a stationary and a rotating disk shrouded by a co-rotating cylinder. *Physics of Fluids* 8, 2605–2613.
- Muite, B.K., 2004. The flow in a cylindrical container with a rotating end wall at small but finite Reynolds number. *Physics of Fluids* 16, 3614–3626.
- Mullin, T., Kobine, J.J., Tavener, S.J., Cliffe, K.A., 2000. On the creation of stagnation points near straight and sloped walls. *Physics of Fluids* 12, 425–431.
- Mununga, L., Hourigan, K., Thompson, M.C., 2004. Confined flow vortex breakdown control using a small rotating disk. *Physics of Fluids* 16, 4750–4753.
- Pao, H.P., 1972. Numerical solution of the Navier–Stokes equation for flows in the disk cylinder system. *Physics of Fluids* 15, 4–11.
- Schmeiden, C., 1928. Über den Widerstand einer Flüssigkeit in einer rotierenden Scheibe. *Zeitschrift für Angewandte Mathematik und Mechanik* 8, 460–479.
- Schultz-Grunow, F., 1935. Der Reibungswiderstand rotierender Scheiben in Gehäusen. *Zeitschrift für Angewandte Mathematik und Physik* 15, 191–204.
- Yu, P., Lee, T.S., Zeng, Y., Low, H.T., 2006. Effects of conoidal lids on vortex breakdown in an enclosed cylindrical chamber. *Physics of Fluids* 18, 117101.
- Yu, P., Lee, T.S., Zeng, Y., Low, H.T., 2007. Characterization of flow behavior in an enclosed cylinder with a partially rotating end wall. *Physics of Fluids* 19, 057104.